Imaging Method for Space Debris Based on GNSS-R

Yuchen Tao*, She Shang

China Academy of Space Technology, Xi'an, China

*Corresponding author: taoyuchen321@163.com

Keywords: GNSS-R, Space debris, Bistatic radar, Narrow band imaging.

Abstract: With the human's exploration activities of space have become increasingly frequent, the amount of space debris increased gradually, this severely affected the spacecraft launch and normal operation. Detection and identification of space debris has become an important task. GNSS-based microwave remote sensing technology has so many advantages due to a low cost and wide coverage, showing broad application prospects in space exploration. This paper studies used navigation satellites as a transmitter, a receiver located in other space platforms, the target reflecting surface scattering coefficient is extracted by using space debris spins Doppler, then an imaging method based on GNSS-R system is proposed to achieve space debris bistatic narrowband imaging. Its effectiveness is verified through the analysis of simulation results it estimated the size of space debris, It is conducive to further space debris detection and classification.

1. Introduction

GNSS-R is a new remote sensing method with low cost, low power consumption and relatively high spatial and temporal resolution by using the reflected signals of navigation satellites. Ground based, airborne and space borne experiments have been carried out for GNSS-R application at home and abroad, and its application field has gradually expanded from ocean remote sensing to land surface remote sensing.

For narrow-band imaging of space debris, rotating Doppler imaging of debris target is used. In recent years, extensive and in-depth research has been carried out at home and abroad. Toru Sato proposed a single range Doppler interferometry (SRDI) [5] algorithm to realize two-dimensional imaging of space debris by using the spin motion of space debris to generate sinusoidal Doppler spectrum. Wang Qi proposed a single range matched filtering (SRMF) algorithm [6]. By constructing matched filters under different rotation radii, the transverse echo data were matched and filtered respectively to obtain the estimation of the scattering intensity of points on different radii, so as to estimate the shape and size of the target. SRMF utilizes fast Fourier transform (FFT) to effectively improve the imaging rate. Compared with SRDI algorithm, SRMF has the advantages of high resolution and less computation.

The research work of this paper is to expand the application of GNSS-R to detect space debris in orbit of spacecraft. Space debris has the characteristics of wide distribution, fast flight speed and strong destructive ability, which seriously affects the launch and normal operation of spacecraft. Therefore, the detection and classification of space debris is an urgent and practical work. Using the navigation satellite as the transmitter and the receiver on other satellite platforms, a narrowband imaging method based on GNSS-R system is presented to obtain the scattering coefficient of the target reflector using the spin Doppler of the spatial fragments. Through the analysis of simulation results, the validity of the algorithm is verified, and the size of spatial fragments is estimated, which is helpful for further detection and classification of spatial fragments. The feasibility of the algorithm is verified by experimental simulation.

2. Signal model for spatial fragmentation

Using high-orbiting navigation satellites as radiation source, the receiver is placed on a vehicle with space debris in close orbit, and the transmitter, receiver and space debris all move at high speed. To simplify the analysis, the space fragments only rotate without translation, and the transmitter and receiver move radially relative to the space fragments.

The template is used to format your paper and style the text. All margins, column widths, line spaces, and text fonts are prescribed; please do not alter them. You may note peculiarities. For example, the head margin in this template measures proportionately more than is customary. This measurement and others are deliberate, using specifications that anticipate your paper as one part of the entire proceedings, and not as an independent document. Please do not revise any of the current designations. As shown in Figure 1, the space debris is centered at the origin, the angular velocity is ω, and it rotates counterclockwise. The transmitter and receiver are located at the scattering center at distances R_T and R_R, and the moving speed is v_T and v_R. The formed double base angle is β. At time t, the distances from the transmitter and receiver to the scattering point P are $R_T(t)$ and $R_R(t)$ respectively, and the double base distance is $R_T(t)+R_R(t)$. The scattering point P is located at (r_k,γ_k), which means that the distance from the center of rotation on the space debris is r_k, and the angle with the X axis is Scattering point of γ_k.

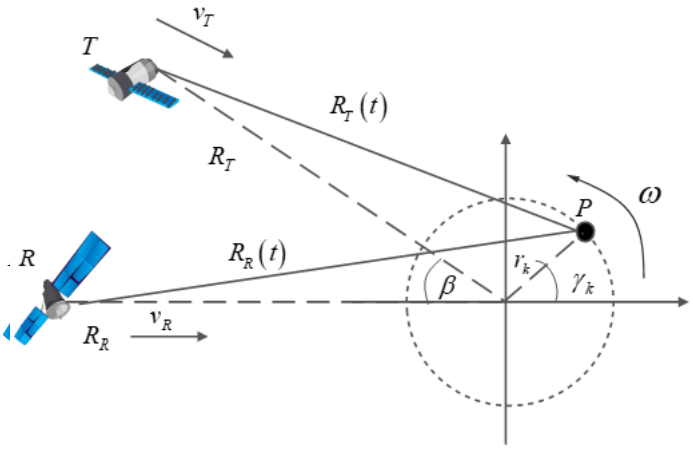

Figure 1. Geometry of bistatic rada.

$$R_R(t)=\sqrt{(R_R-v_Rt)^2+r_k^{\,2}-2r(R_R-v_Rt)\cos(\omega t+\gamma_k)}\approx R_R-v_Rt-r_k\cos(\omega t+\gamma_k) \tag{1}$$

$$R_T(t)=\sqrt{(R_T-v_Tt)^2+r^2-2r(R_T-v_Tt)\cos(\omega t+\gamma-\beta)}\approx R_T-v_Tt-r_k\cos(\omega t+\gamma_k-\beta) \tag{2}$$

$$R_k(t)=R_R(t)+R_T(t)=R_0+v_rt+r'\cos(\omega t+\gamma_k-\beta/2) \tag{3}$$

Where, $v_r=-(v_R+v_T)$, $r_k'=-2\cdot r_k\cos(\beta/2)$ the band modulation signal of the navigation signal is a periodic pseudo-random sequence, and the navigation message data is modulated at the same time in the signal, which is up-converted and modulated by the carrier frequency. The transmission signal expression of a typical navigation satellite is shown in (4):

$$s(t)=A_cC(t)D(t)\sin(2\pi f_ct+\phi) \tag{4}$$

Where, A_c, $C(t)$, $D(t)$, f_c and ϕ are signal amplitude, pseudo-random code, navigation message, carrier frequency and initial carrier phase. In (4) Imaging does not require navigation messages, Ignore message modulation by processing. Echo signal is a transmitted signal that has been attenuated and delayed and can be written in (5):

$$s_r(t)=\sum_{k=1}^{K}\alpha_k A_c C\left(t-\tau_k(t)\right)\sin\left(2\pi f_c\left(t-\tau_k(t)\right)+\phi\right) \tag{5}$$

Where, α_k , $\tau_k(t)$ represent the amplitude attenuation factor and transmission delay time corresponding to the *k*th target in the spatial fragment of the echo signal. The expression of the signal after the echo signal is converted to the baseband by down-conversion and orthogonal demodulation is shown in (6):

$$s_b(t)=\sum_{k=1}^{K}\alpha_k A_c C\left(t-\tau_k(t)\right)\exp\left(-j2\pi f_c\tau_k(t)\right) \tag{6}$$

The common imaging algorithms are pulse signals, and the imaging processing is generally two-dimensional signals. Navigation signal is continuous wave signal, so it is necessary to divide one-dimensional original signal into two-dimensional time-domain signal. In theory, any time interval can be used as the equivalent pulse repetition interval to divide the fast and slow time. However, in actual operation, it is also necessary to consider the influence of the block length on the peak sidelobe ratio of the range pulse compression, range blur, Doppler aliasing, and imaging processing effects [7]. Duty ratio of continuous wave signal is 1, after dividing the pulse repetition interval, the equivalent pulse repetition frequency and the equivalent pulse width will be reciprocal. Taking GPS signal as an example, the repetition period of C/A code is 1ms, so it is a reasonable way to use 1ms as the equivalent pulse repetition interval for two-dimensional block processing. At this time, the equivalent PRF (pulse repetition rate) is 1000 Hz. After the division of fast and slow time, one-dimensional discrete signal can be transformed into two-dimensional matrix.

$$\begin{aligned} &s_b\left(\hat{t},t_m\right)\\ &\quad=\sum_{k=1}^{K}\alpha_k A_c C\left(t_m+\hat{t}-\tau_k\left(\hat{t}+t_m\right)\right)\exp\left(-j2\pi f_c\tau_k\left(\hat{t}+t_m\right)\right) \end{aligned} \tag{7}$$

In (5), where $\hat{t}$, t_m are fast time and slow time respectively. $0\le t_m\le T_c$, $0\le\hat{t}\le T_s$, $\hat{t}=t-t_m$, where t is whole time, T_c is observed time, T_s is PRI(pulse repetition interval). It can be seen from (7) that the delay and Doppler phase are both functions of fast and slow time, but there is a significant difference between the time delay and Doppler simulation results analysis of the phase change over time. The time delay can be approximated as slow time change, and the Doppler phase needs to consider changes by fast time. After adopting the above approximation, the expression of the echo signal can be further simplified as (8):

$$s_{Echo}\left(\hat{t},t_m\right)=\sum_{k=1}^{K}\alpha_k A_C C\left(\hat{t}-\tau_k\left(t_m\right)\right)\cdot\exp\left(-j\varphi_k\left(\hat{t}+t_m\right)\right) \tag{8}$$

Where $\varphi_k\left(t_m+\hat{t}\right)$ is Doppler phase of echo signal?

3. Doppler phase of echo signal.

Since bistatic platforms are moving at high speeds, Doppler frequency deviation is generated, and the pulse compression of the navigation signal is sensitive to Doppler, so Doppler frequency compensation is necessary. Firstly, the analysis platform generates Doppler for analysis.

Where, $f_{dt}=2v_r/\lambda$, $f_{dr}=2r_k'w\cos(wt)/\lambda$, f_{dt} is translational Doppler frequency, f_{dr} is rotational Doppler frequency, and $f_{dt}\gg f_{dr}$. For phase coded signals, pulse compression is greatly affected by translational Doppler, which mainly compensates the Doppler frequency generated by translational motion. The multi-channel Doppler compensation algorithm is adopted, and the code serial carrier parallel search method is adopted [8]. As shown in Fig.2, a single symbol generator is used to search the code in serial, N_f carrier correlators are used to search the carrier translation Doppler. The local code is moved one code phase unit (usually half a chip) at one time, the shift signal is correlated with

the received signal, and the path with the largest peak side lobe ratio is selected, and the corresponding code phase and carrier frequency values are recorded for subsequent signal pulse compression.

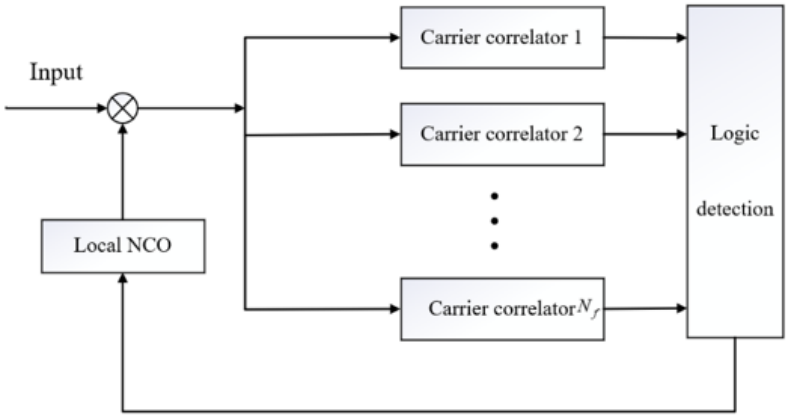

Figure 2. Doppler frequency offset estimation.

N_f carrier correlators generate carriers of different frequencies, the number of which is related to the search range and search step. The search step mainly considers the Doppler tolerance of phase-coded signals, when $f_d T \ll 1/4$, the influence of Doppler frequency shift on pulse pressure effect is not considered, so the search step meets $\Delta f_d T \ll 1/4$.Therefore, after frequency offset compensation:

$$f_d' = f_d - \hat{f}_d \approx f_{dr} \tag{9}$$

Because the Doppler f_d' changes slightly with respect to fast time after compensation, which is equivalent to only rotating Doppler, the effect on pulse compression can be ignored, so the phase change caused by Doppler can be regarded as a change with slow time.

$$s_b\left(t_m,\hat{t}\right)=\sum_{k=1}^{K}\alpha_k A_c C\left(t_m+\hat{t}-\tau_k(t_m)\right)\exp\left(-\mathrm{j}\varphi_k\left(t_m\right)\right) \tag{10}$$

$$\varphi_k\left(t_m\right)=\frac{2\pi\left(R_0+r_k'\cos\left(\omega t_m+\gamma_k-\beta/2\right)\right)}{\lambda} \tag{11}$$

After the Doppler frequency shift compensation is completed, the compensated signal is pulse compressed. Where $p(t)$ is the pseudocode correlation of the navigation signal? Compressed output?

$$s_b\left(t_m,\hat{t}\right)=\sum_{k=1}^{K}\alpha_k A_c p\left(t_m+\hat{t}-\tau_k(t_m)\right)\exp\left(-\mathrm{j}\varphi_k\left(t_m\right)\right) \tag{12}$$

From the above formula, it can be seen that due to the high-speed movement of the receiving, sending platforms and targets, the target location will appear in multiple distance units during the observation time, which has a great impact on the subsequent extraction of rotating Doppler. In addition, the size of spatial fragments is small, and the scattering points should be within the same distance gate. Envelope alignment is necessary before imaging. Common distance alignment methods include peak method, maximum correlation method, frequency domain method [9], Hoff transformation method [10] and minimum entropy method [11]. These methods are applicable to cases where the translational priori knowledge is unknown. The maximum correlation method used in this paper. After envelope alignment, take out the data of the distance unit where the target is located:

$$\begin{aligned} s_c\left(t_m\right)&=\sum_{k=1}^{K}\mathrm{A}\cdot\mathrm{rect}\left(\frac{t_m}{T_c}\right)\exp-\left(\mathrm{j}\frac{2\pi\left(R_0+r_k'\sin\left(\omega t_m+\gamma_k-\beta/2\right)\right)}{\lambda}\right)\\ &=\sum_{k=1}^{K}\mathrm{A}'\cdot\mathrm{rect}\left(\frac{t_m}{T_c}\right)\exp\left(-\mathrm{j}\frac{2\pi r_k'\sin\left(\omega t_m+\gamma_k-\beta/2\right)}{\lambda}\right)\end{aligned} \tag{13}$$

Where $A' = A \cdot \exp(-2\pi R_0 / \lambda)$, Equivalent to a constant. From the above formula, it can be seen that the time-frequency distribution of the azimuth of the motion compensated echo signal compressed in a distance unit under narrow band conditions is periodic sinusoidal distribution.

4. SRMF imaging algorithm

Assuming that the angular velocity of self-rotation of spatial fragments is constant during observation time, the transverse echo is the sum of a series of known waveforms with different rotation radii *r* and angular phase γ as variable parameters. If we give a polar coordinate position (*r*, γ) of a point, we can establish the theoretical echo waveform of the point. Taking the signal waveform of the point as the reference signal, we can get the impulse response of the scattering point by adding the transverse echo phase correction for coherent processing. When the point is selected to realize coherent integration, the filtered output signal of the point near the point will not be completely coherent, which will reduce the amplitude of the output signal and only focus on the point. The impulse response of each scattering point with different radius and angle can be obtained in turn, and the complete two-dimensional image of the target can be obtained finally. It needs to be pointed out that the amount of computation for direct matching filter through convolution is relatively large. The convolution between the signal and the matched filter can be obtained by FFT through conjugate multiplication in frequency domain and IFFT, which greatly improves the operation efficiency. The echo signal of equation (13) is transformed into frequency domain by Fourier transform to discuss how to deal with it, the echo FFT becomes:

$$S(f) = \sum_i \int_{T_1}^{T_2} A_i \exp\left[-\frac{j4\pi}{\lambda} r_i \sin(\omega\tau + \gamma_i)\right] \exp(-j2\pi f\tau) d\tau \tag{14}$$

Where $[T_1, T_2]$ is the sampling interval, The r_k reference matching signal is established for each rotation radius r_k, $r_k \in (0, r_{\max})$:

$$S_{ref}^k(f) = \exp\left[-j4\pi r_k \sin(\omega\tau)\right] \tag{15}$$

After FFT of reference signal of (15):

$$S(f) = \sum_i \int_{T_1+\frac{\gamma}{\omega}}^{T_2+\frac{\gamma}{\omega}} A_i \exp\left[-\frac{j4\pi}{\lambda} r_i \sin(\omega t_1)\right] \exp(-j2\pi f t_1) \exp\left(-j2\pi f \frac{\gamma_i}{\omega}\right) dt_1 \tag{16}$$

Let $t_1 = \tau - \frac{\gamma_i}{\omega}$, then (15) is transformed into:

$$S(f) = \sum_i \int_{T_1+\frac{\gamma}{\omega}}^{T_2+\frac{\gamma}{\omega}} A_i \exp\left[-\frac{j4\pi}{\lambda} r_i \sin(\omega t_1)\right] \exp(-j2\pi f t_1) \exp\left(-j2\pi f \frac{\gamma_i}{\omega}\right) dt_1 \tag{17}$$

Generally, the sampling points of periodic signal should include integer period, otherwise spectrum leakage will occur, which will bring adverse effects. On the basis of self-rotation period obtained by autocorrelation method, it is easy to select integer multiple period data, $\omega(T_2 - T_1) = 2k\pi$, $k = 1, 2, \cdots$ From this we can get

$$S(f) = \sum_i \int_{T_1}^{T_2} A_i \exp\left[-\frac{j4\pi}{\lambda} r_i \sin(\omega t_1)\right] \exp(-j2\pi f t_1) dt_1 \exp\left(-j2\pi f \frac{\gamma_i}{\omega}\right) \tag{18}$$

When the reference signal of radius r_k is matched and filtered, the echoes on other radii are regarded as clutter, and there are *p* scattering points on the radius r_k, let:

$$S(f) = \sum_i \int_{T_1}^{T_2} A_i \exp\left[-\frac{j4\pi}{\lambda} r_i \sin(\omega t_1)\right] \exp(-j2\pi f t_1) dt_1 \exp\left(-j2\pi f \frac{\gamma_i}{\omega}\right) + n = S_k(f) + n \tag{19}$$

In equation (19), *n* is the contribution of the sum of the echoes except the signal on the radius of rotation r_k . The relative reference signal is regarded as clutter, and it will not form a completely coherent output after matching with the reference signal. The frequency domain of the signal on the radius of rotation r_k is as follows:

$$S_k(f)=\sum_p A_p S_{ref}(f)\exp\left(-j2\pi f\frac{\gamma_p}{\omega}\right) \tag{20}$$

After matched filtering, the influence of clutter is ignored:

$$s(t)=F_{(f)}^{-1}\left[S(f)S_{ref}^{*}(f)\right]=F_{(f)}^{-1}\left[\sum_p A_p S_{ref}(f)S_{ref}^{*}(f)\exp\left(-j2\pi f\frac{\gamma_p}{\omega}\right)\right] \tag{21}$$

Finally, the signal output expression with the radius of rotation r_k is obtained:

$$s(t)=\sum_p A_p\, psf\left(t-\frac{\gamma_p}{\omega}\right) \tag{22}$$

Where $psf(t)=F_{(f)}^{-1}\left[\left|S_{ref}(f)\right|^2\right]$, $psf(\bullet)$is Point Spread Function? Therefore, the scattering intensity of each point above the radius of rotation r_k can be obtained by the above steps. The position estimation of scattering points on each radius can be obtained by matching the filtered reference signal with different rotation radius, and then the two-dimensional image of the rotating target can be obtained.

5. Simulation results analysis

Table 1. Simulation parameter table.

parameter	transmitter	Receiver
distance/km	150	100
radial velocity /m*s^{-1}	1000	1000
Bistatic angle /degree	30	
SNR/dB	0	

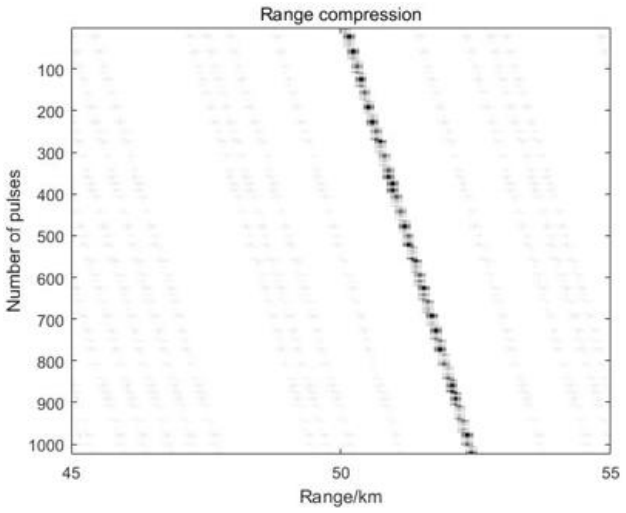

Figure 3. Before envelope alignment.

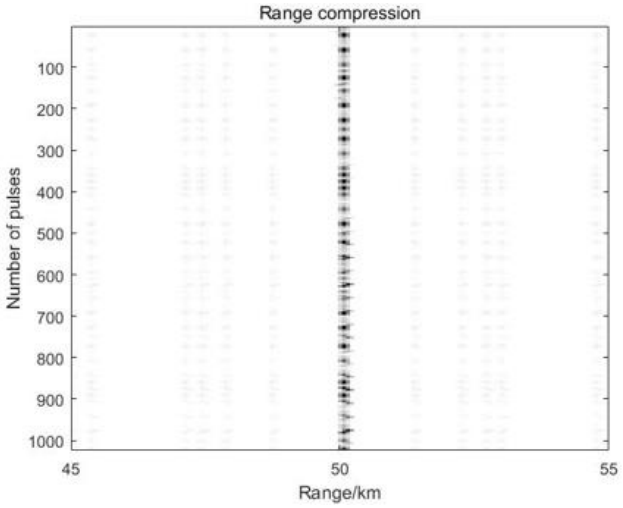

Figure 4. After envelope alignment.

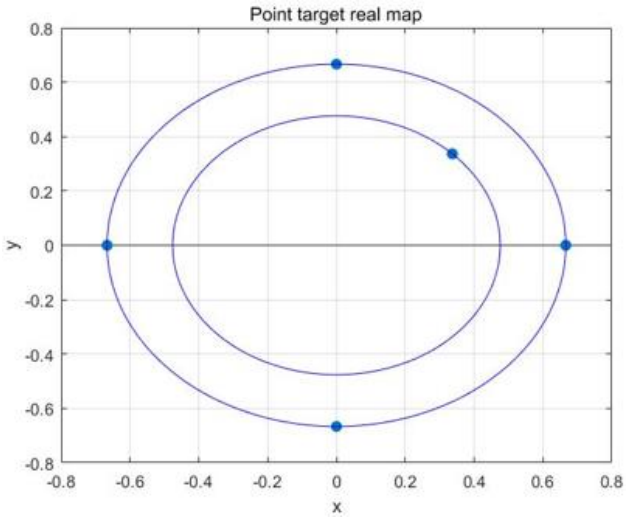

Figure 5. Reallocation of target.

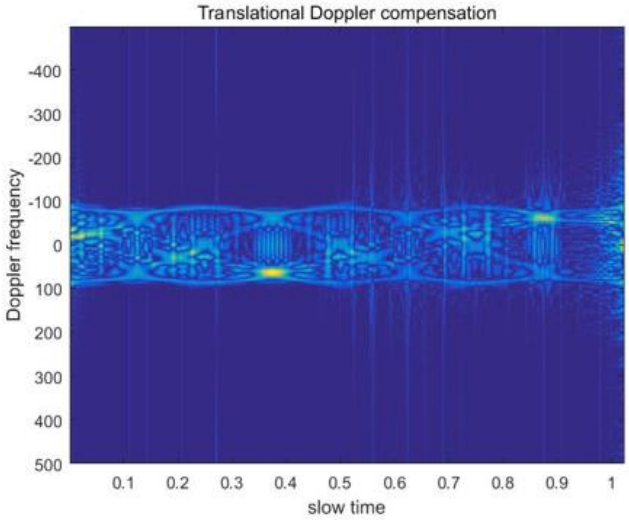

Figure 6. Time frequency distribution of Spinning Target.

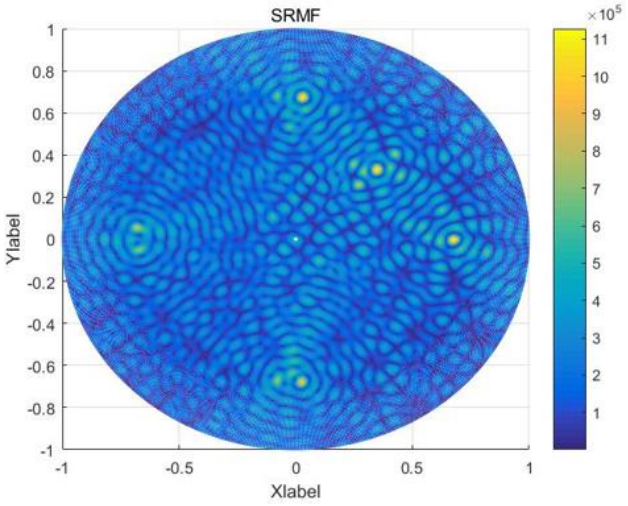

Figure 7. 2-D imaging results.

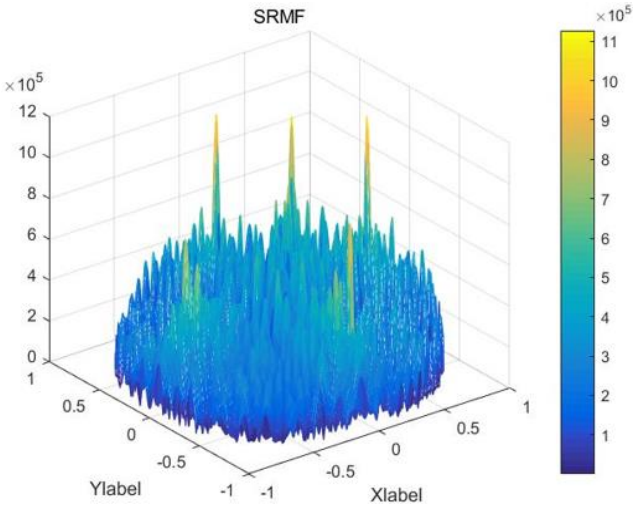

Figure 8. 3-D imaging results.

6. Conclusion

In this paper, the bistatic imaging method for space debris in GNSS-R system is studied, and an imaging method suitable for navigation signal is proposed. Firstly, Doppler compensation is used to solve the problem that the pulse pressure of navigation signal is sensitive to Doppler. Secondly, the maximum correlation method is used to align the envelope of the target moving across the range gate, and then the range gate data of the target are extracted. Finally, the spin motion of space debris is used to generate a sinusoidal Doppler spectrum, and a single range matching filter is used to image the space debris. The feasibility of this method is verified by the processing results of simulation data.

References

[1] Li Huang, Xia Qing, and Yin Cong Wan Wei, The Current Status of Research on GNSS-R Remote Sensing Technology in China and Future Development, Journal of Radars, 2013, 12(2):389-399.

[2] Cherniakov M, Saini R, Zuo R, et al. Space surface Bistatic SAR with space-borne non-cooperative transmitters[C].European Radar Conference, France, 2005: 9-12.

[3] Antoniou M, Saini R, and Cherniakov M. Results of a space-surface bi-static SAR image formation algorithm [J].IEEE Transactions on Geoscience and Remote Sensing, 2007, 45(11): 3359-3371.

[4] Tian Weiming, Hu Shanqing, and Zeng Tao. A frequency synchronization scheme based on PLL for BiSAR and experiment result[C]. International Conference on Signal Processing, 2008: 2425-2428.

[5] T. Sato, “Shape estimation of space debris using single-range Doppler interferometry,” IEEE Trans. Geosci. Remote Sens., vol.37, no.2, pp. 1000-1005, 1999.

[6] Li Huang, Xia Qing, and Yin Cong Wan Wei, The Current Status of Research on GNSS-R Remote Sensing Technology in China and Future Development, Journal of Radars, 2013, 12(2):389-399.

[7] Tian Weiming, Hu Shanqing, and Zeng Tao. BISAR imaging technology based on navigation signal [J], Journal of Radars, 2013, 3 (2):39-45

[8] Yang Dongkai, Zhang Qishan. GNSS reflection signal processing foundation and Practice [M], Publishing House of Electronics Industry, 2012:46.

[9] Tian Weiming, Hu Shanqing, and Zeng Tao. BISAR imaging technology based on navigation signal [J], Journal of Radars, 2013, 3 (2):39-45

[10] Tian Weiming, Hu Shanqing, and Zeng Tao. BISAR imaging technology based on navigation signal [J], Journal of Radars, 2013, 3 (2):39-45

[11] X. Li, G. Liu and J. Ni. Autofocusing of ISAR images based on entropy minimization. IEEE Trans. on AES, 1999, 35 (4):1240-1251.

[12] Mikhail Cherniakov. Bistatic Radar Emerging Technology [M].John Wiley & Sons Ltd, 2007.